

Problem 1

A two-dimensional cavity is filled with an incompressible Newtonian fluid. The fluid is driven by the lid moving with a constant velocity U . The cavity has dimensions $H \times H$. Find the steady state solution.

- (a) Solve the above problem using the artificial compressibility method. Describe the essential steps in physical terms, explaining why it can be used to model an incompressible fluid. Detail the computational grid you chose as well as the spatial and temporal discretization. State your boundary conditions and how they were implemented.

0.1 Artificial Compressibility Method

We want to solve the incompressible flow but the density is constant. Meaning, there is no correlation between density and pressure. This makes it unsolvable as-is. In compressible flow, the density can be determined from the continuity equation. Therefore, if we modify the equation of state for the incompressible flow, replacing density with the equation for pressure, we can solve for pressure. This is the basic idea behind the Artificial Compressibility Method. The method will work with only steady state problems, not time-dependent flow. The method is as follows.

The continuity equation for an incompressible fluid:

$$\frac{\partial u}{\partial x} + \frac{\partial v}{\partial y} = 0 \quad (1)$$

We now introduce an artificial equation of state by using the artificial density $\tilde{\rho}$, pressure p , and artificial compressibility constant β :

$$p = \frac{\tilde{\rho}}{\beta} \quad (2)$$

The continuity equation is modified using the artificial time \tilde{t} :

$$\frac{\partial \tilde{\rho}}{\partial \tilde{t}} + \frac{\partial u}{\partial x} + \frac{\partial v}{\partial y} = 0 \quad (3)$$

This works when solving for steady state because $\frac{\partial \tilde{\rho}}{\partial \tilde{t}} = 0$ at steady state. When solving the problem explicitly, we define the artificial speed of sound $\tilde{a} = \frac{1}{\sqrt{\beta}}$, the Mach number $M = \frac{v_{max}}{\tilde{a}} < 1$, and the artificial time step $\Delta \tilde{t} < \Delta x \beta^{1/2}$. Let us now introduce the transport equations on which the Artificial Compressibility Method will be implemented.

0.2 Transport Equations

The u -momentum equation:

$$\frac{\partial u}{\partial \tilde{t}} + \left(\frac{\partial u^2}{\partial x} + \frac{\partial uv}{\partial y} \right) = -\frac{\partial p}{\partial x} + \frac{1}{Re} \left(\frac{\partial^2 u}{\partial x^2} + \frac{\partial^2 u}{\partial y^2} \right) \quad (4)$$

The v -momentum equation:

$$\frac{\partial v}{\partial \tilde{t}} + \left(\frac{\partial uv}{\partial x} + \frac{\partial v^2}{\partial y} \right) = -\frac{\partial p}{\partial y} + \frac{1}{Re} \left(\frac{\partial^2 v}{\partial x^2} + \frac{\partial^2 v}{\partial y^2} \right) \quad (5)$$

The continuity equation:

$$\frac{\partial p}{\partial \tilde{t}} + \frac{1}{\beta} \frac{\partial u}{\partial x} + \frac{1}{\beta} \frac{\partial v}{\partial y} = 0 \quad (6)$$

These equations will be discretized to explicitly solve for steady state. Forward differences will be used for temporal discretization and central differences will be used for spatial discretization. In the 2D grid, let i represent the element index for the x -direction (columns) and j represent the element index for the y -direction (rows). Let n represent the time-step index. The time step is Δt and the grid spacing is $h = \Delta x = \Delta y$.

0.3 Discretization of u-momentum

$$\frac{\partial u}{\partial \tilde{t}} \leftarrow \frac{u_{i,j}^{n+1} - u_{i,j}^n}{\Delta t} \quad (7)$$

$$C_u = \left(\frac{\partial u^2}{\partial x} + \frac{\partial uv}{\partial y} \right) \leftarrow \frac{(u_{i+1,j}^n)^2 - (u_{i-1,j}^n)^2}{2\Delta x} + \frac{u_{i,j+1}^n v_{i,j+1}^n - u_{i,j-1}^n v_{i,j-1}^n}{2\Delta y} \quad (8)$$

$$P_u = -\frac{\partial p}{\partial x} \leftarrow -\frac{p_{i+1,j}^n - p_{i-1,j}^n}{2\Delta x} \quad (9)$$

$$D_u = \frac{1}{Re} \left(\frac{\partial^2 u}{\partial x^2} + \frac{\partial^2 u}{\partial y^2} \right) \leftarrow \frac{1}{Re} \left(\frac{u_{i+1,j}^n - 2u_{i,j}^n + u_{i-1,j}^n}{(\Delta x)^2} + \frac{u_{i,j+1}^n - 2u_{i,j}^n + u_{i,j-1}^n}{(\Delta y)^2} \right) \quad (10)$$

The u -momentum equation can be written in terms of advection C_u , pressure P_u , and diffusion D_u :

$$\frac{u_{i,j}^{n+1} - u_{i,j}^n}{\Delta t} + C_u = P_u + D_u \quad (11)$$

We can use this to solve for the x -velocity u at the next time step:

$$u_{i,j}^{n+1} = u_{i,j}^n + \Delta t(P_u + D_u - C_u) \quad (12)$$

0.4 Discretization of v-momentum

$$\frac{\partial v}{\partial \tilde{t}} \leftarrow \frac{v_{i,j}^{n+1} - v_{i,j}^n}{\Delta t} \quad (13)$$

$$C_v = \left(\frac{\partial uv}{\partial x} + \frac{\partial v^2}{\partial y} \right) \leftarrow \frac{u_{i+1,j}^n v_{i+1,j}^n - u_{i-1,j}^n v_{i-1,j}^n}{2\Delta x} + \frac{(v_{i,j+1}^n)^2 - (v_{i,j-1}^n)^2}{2\Delta y} \quad (14)$$

$$P_v = -\frac{\partial p}{\partial y} \leftarrow -\frac{p_{i,j+1}^n - p_{i,j-1}^n}{2\Delta y} \quad (15)$$

$$D_v = \frac{1}{Re} \left(\frac{\partial^2 v}{\partial x^2} + \frac{\partial^2 v}{\partial y^2} \right) \leftarrow \frac{1}{Re} \left(\frac{v_{i+1,j}^n - 2v_{i,j}^n + v_{i-1,j}^n}{(\Delta x)^2} + \frac{v_{i,j+1}^n - 2v_{i,j}^n + v_{i,j-1}^n}{(\Delta y)^2} \right) \quad (16)$$

The v -momentum equation can be written in terms of advection C_v , pressure P_v , and diffusion D_v :

$$\frac{v_{i,j}^{n+1} - v_{i,j}^n}{\Delta t} + C_v = P_v + D_v \quad (17)$$

We can use this to solve for the y -velocity v at the next time step:

$$v_{i,j}^{n+1} = v_{i,j}^n + \Delta t(P_v + D_v - C_v) \quad (18)$$

0.5 Discretization of the Continuity Equation

$$\frac{\partial p}{\partial \tilde{t}} \leftarrow \frac{p_{i,j}^{n+1} - p_{i,j}^n}{\Delta t} \quad (19)$$

$$\frac{1}{\beta} \frac{\partial u}{\partial x} \leftarrow \frac{1}{\beta} \frac{u_{i+1,j}^n - u_{i-1,j}^n}{2\Delta x} \quad (20)$$

$$\frac{1}{\beta} \frac{\partial v}{\partial y} \leftarrow \frac{1}{\beta} \frac{v_{i,j+1}^n - v_{i,j-1}^n}{2\Delta y} \quad (21)$$

Solving the continuity equation for pressure at the next time step, we get:

$$p_{i,j}^{n+1} = p_{i,j}^n - \frac{\Delta t}{\beta} \left(\frac{u_{i+1,j}^n - u_{i-1,j}^n}{2\Delta x} + \frac{v_{i,j+1}^n - v_{i,j-1}^n}{2\Delta y} \right) \quad (22)$$

0.6 Boundary Conditions

The velocity in the x -direction u is U at the top wall $y = H$ and zero at the other walls $x = 0$, $x = H$, and $y = 0$. The velocity in the y -direction v is zero at all walls $x = 0$, $x = H$, $y = 0$, and $y = H$. These are the no-slip boundary conditions.

Since there is no flow across the boundaries, pressure inside the boundary is equal to the pressure outside the boundary such that $\frac{\partial p}{\partial x} = 0$ at the left/right walls and $\frac{\partial p}{\partial y} = 0$ at the top/bottom walls. These are our Neumann boundary conditions.

At the left wall $x = 0$ and right wall $x = H$ we have:

$$\left(\frac{\partial p}{\partial x} \right)_i = \frac{p_{i+1,j}^n - p_{i-1,j}^n}{2\Delta x} = 0 \quad (23)$$

Such that our boundary condition is:

$$p_{i+1,j}^n = p_{i-1,j}^n \quad (24)$$

For example, at $i = 0$ we get $p_{0,j} = \frac{p_{1,j} + p_{-1,j}}{2} = p_{1,j}$ and at $i = N - 1$ we get $p_{N-1,j} = \frac{p_{N,j} + p_{N-1,j}}{2} = p_{N-2,j}$.

At the top wall $y = H$ and bottom wall $y = 0$ we have:

$$\left(\frac{\partial p}{\partial y} \right)_j = \frac{p_{i,j+1}^n - p_{i,j-1}^n}{2\Delta y} = 0 \quad (25)$$

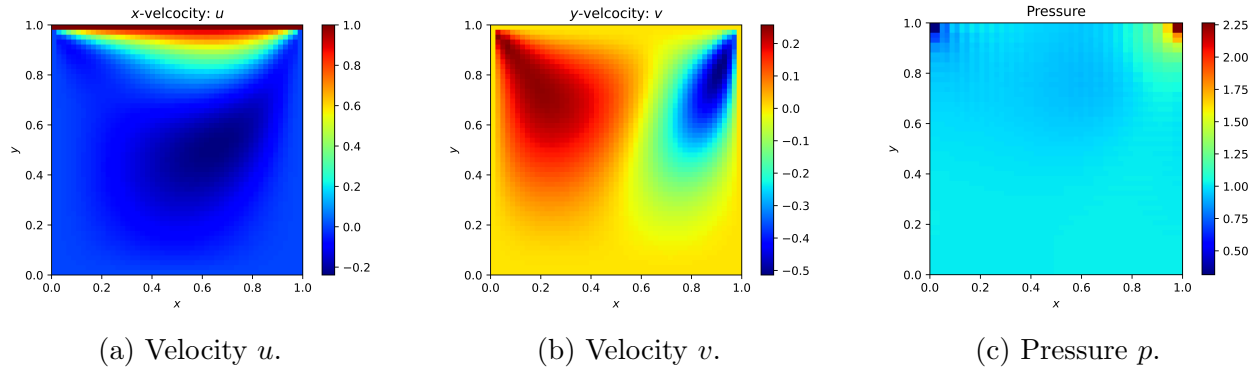
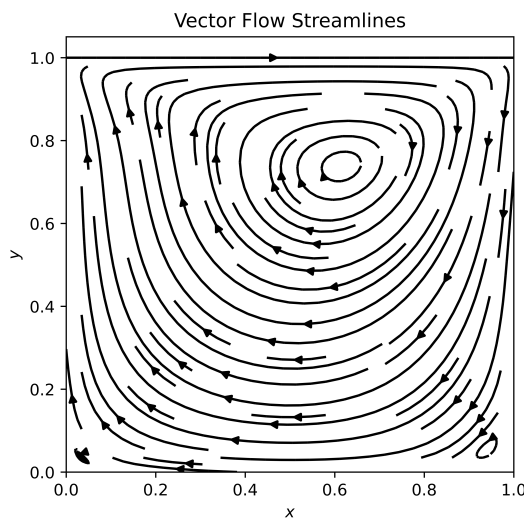
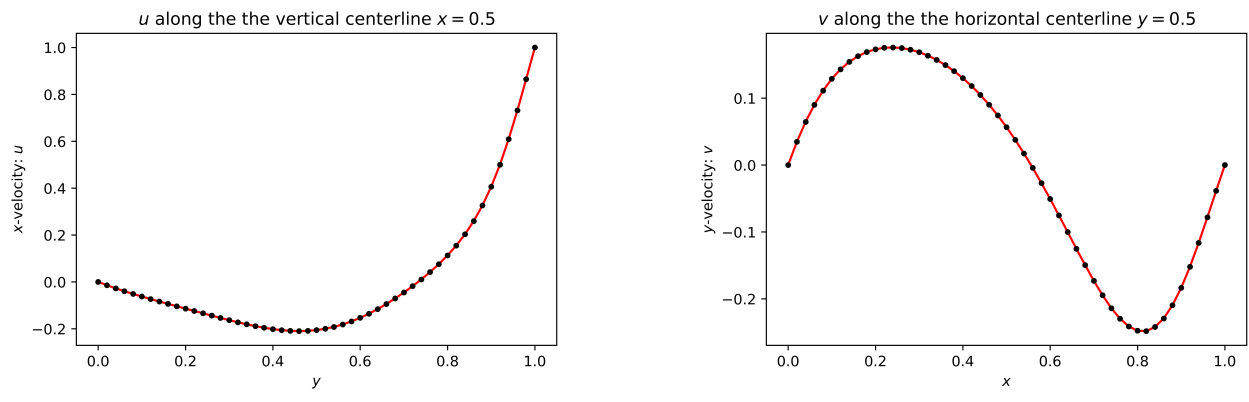
Such that our boundary condition is:

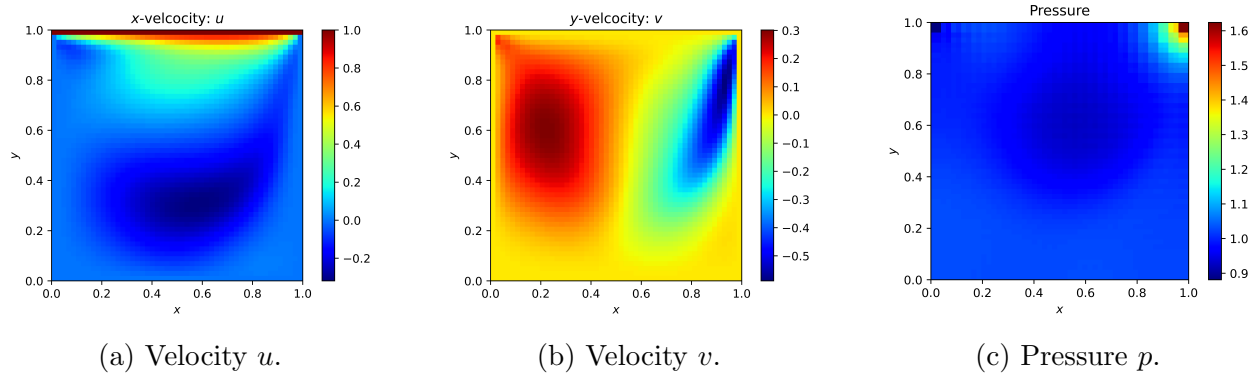
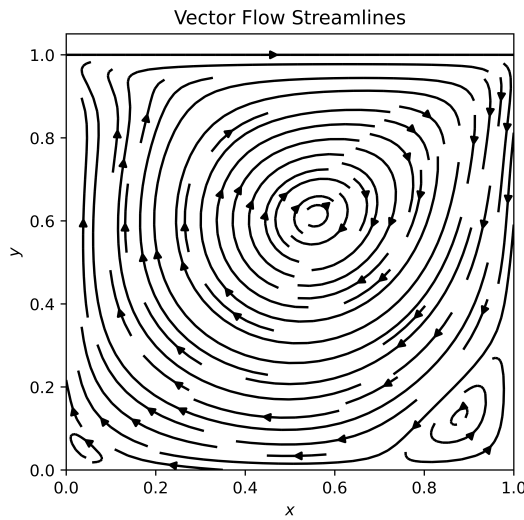
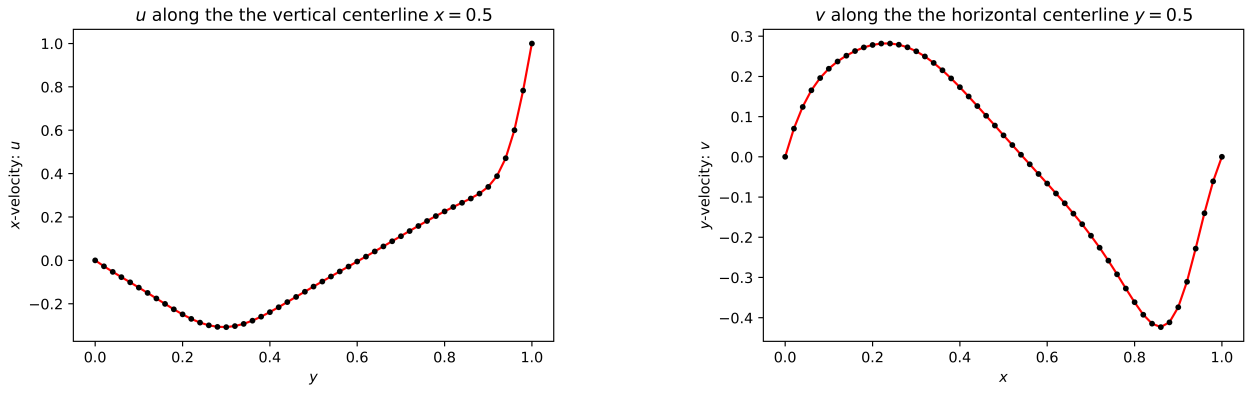
$$p_{i,j+1}^n = p_{i,j-1}^n \quad (26)$$

Therefore, at $j = 0$ we get $p_{i,0} = p_{i,1}$ and at $j = N - 1$ we get $p_{i,N-1} = p_{i,N-2}$.

- (b) Consider a square cavity. In this problem the Reynolds number, defined by $Re = UH/\nu$, characterizes the flow patterns. Compute the steady state solutions for both $Re = 100$ and $Re = 400$. State your steady state criteria (it should use all points in the domain). Plot the steady state streamlines. Plot the x-component of velocity along the vertical centerline. Plot the y-component of velocity along the horizontal centerline. Compare your results to those found in the literature.

0.7 Simulation Results

Figure 1: Steady state u, v, p grids at $Re = 100$.Figure 2: Steady state streamlines at $Re = 100$.Figure 3: Steady state u and v at $Re = 100$.

Figure 4: Steady state u, v, p grids at $Re = 400$.Figure 5: Steady state streamlines at $Re = 400$.Figure 6: Steady state u and v at $Re = 400$.

0.8 Simulation Criteria

The initial conditions of the simulation are as follows:

Velocity u : $U = 1$ at the lid, zero elsewhere

Velocity v : zero everywhere

Pressure p : $P = 1$ everywhere

Domain $H = 1$

$N = 51$ grid points in either direction

$h = \Delta x = \Delta y = 0.02$

$\Delta t = 0.001$

$\beta = 2.5$

Whether the solution has converged to steady state depends on the change in the u and v velocities with time.

$$e_{ij} = \frac{\partial u}{\partial t} + \frac{\partial v}{\partial t} = \frac{u_{ij}^{n+1} - u_{ij}^n + v_{ij}^{n+1} - v_{ij}^n}{\Delta t} \quad (27)$$

We take the L2 norm over all e_{ij} on the grid as the error measurement.

$$\epsilon = \sqrt{\sum_{i,j} e_{ij}^2} \quad (28)$$

The convergence criteria for the above solutions is $\epsilon < 10^{-10}$. For reference, the error during the first few iterations have the order of magnitude 10^{-5} and 10^{-6} at $Re = 100$ and $Re = 400$, respectively.

0.9 Comparison to Literature

The steady state streamlines for $Re = 100$ (Fig.2) and $Re = 400$ (Fig.5) look similar to those in the resource. From $Re = 100$ to $Re = 400$, the main vortex shifts downward and the vortices in the bottom corners of the cavity become larger.

We define the minimum velocity at the vertical centerline as u_{min} , the minimum velocity at the horizontal centerline as v_{max} , and the maximum velocity at the horizontal centerline as v_{max} (See Figures 3 and 6). These values are compared to the literature values in Table 1, where percent error is defined as:

$$\delta = \frac{|simulation - resource|}{|resource|} \times 100\% \quad (29)$$

Overall, the simulation results are representative of those in the resource. At $Re=100$, the simulation values are accurate with an overall percent error of less than two-percent.

On the other hand, at $Re=400$, the simulation values are less accurate with an overall percent error of less than seven-percent. These errors could be improved by reducing truncation error through increasing the grid size. The higher Reynolds solution may have larger percent error because it takes longer to converge and may require smaller criteria for convergence to be more representative of the solution in the resource.

Velocity	Re	Simulation	Resource	% Error
u_{min}	100	-0.21003	-0.21090	0.4%
v_{min}	100	-0.24832	-0.24533	1.2%
v_{max}	100	0.17568	0.17527	0.2%
u_{min}	400	-0.30790	-0.32726	5.9%
v_{min}	400	-0.42353	-0.44993	5.9%
v_{max}	400	0.28188	0.30203	6.7%

Table 1: Comparison of simulation and resource values for u_{min} , v_{min} , and v_{max} .

Resource: Ghia, U. K. N. G., Kirti N. Ghia, and C. T. Shin. “High-Re solutions for incompressible flow using the Navier-Stokes equations and a multigrid method.” *Journal of computational physics* 48.3 (1982): 387-411.

(c) **Describe the main features of the flow. How does the flow change with Re ?**

There is a primary clockwise vortex that is formed due to the velocity of the lid. Since the lid is moving in the positive x -direction (left to right), liquid accumulates along the right wall, pushing the fluid downward. This is visible in the plots of v in which the right part of the cavity has a largely negative velocity whereas the velocity is largely positive on the left side. Due to this combination of v velocity direction changing along the horizontal axis of the cavity, along with the slight shift in u velocity from positive to negative, the primary vortex is formed. Vortices are also formed at the bottom corners of the cavity due to the no-slip boundary conditions. These are counter-clockwise due to the combination of no-slip at the corners with the direction of the streamline along the outside edge of the primary vortex.

Since Reynolds number Re characterizes the ratio of inertial forces to viscous forces, higher Re signifies that the inertial forces are more significant i.e. the flow is more susceptible to changes in velocity. As seen in the steady state u and v grids, an increase in Re slightly increases the range of velocities. Thus, with faster velocities, aka more powerful inertial forces, the vortices in the bottom corners become larger and the primary vortex shifts toward the center (pushes away from the lid), such that it is more symmetric with the square cavity center.

(d) **Discuss the stability criteria of the method. How was your time step chosen?**

Recall from part (a) that the artificial time step must agree with the relationship $\tilde{\Delta t} < \Delta x \beta^{1/2}$. Since $\Delta x = 0.02$ and $\beta = 2.5$, we get $\tilde{\Delta t} < 0.03$. The time step that was selected was $\Delta t = 0.001$ because it agrees with this relationship and is small to ensure the Mach number is less than one. This is because the time step of v involves a multiplication by Δt , such that the maximum v will be larger for larger Δt . The quantity v_{max} must be smaller than the artificial speed of sound $\tilde{a} = \frac{1}{\sqrt{\beta}}$ to ensure the Mach number is less than one. In the steady state grids for v , we can see that this relationship is satisfied since $v_{max} < 0.6$.

- (e) For $Re = 100$ and $Re = 400$, qualitatively show your two velocity profiles are converging to the literature values by considering three different grid sizes with the grid resolution doubled each time.

The simulations were executed at $N = \{16, 32, 64\}$ grid points in either direction with a 0.0001 time step, $\beta = 2.5$, and $\epsilon < 10^{-10}$ as the convergence criteria. The following plots show a comparison of velocity profile values u_{min} , u_{max} , and v_{max} with those from the literature.

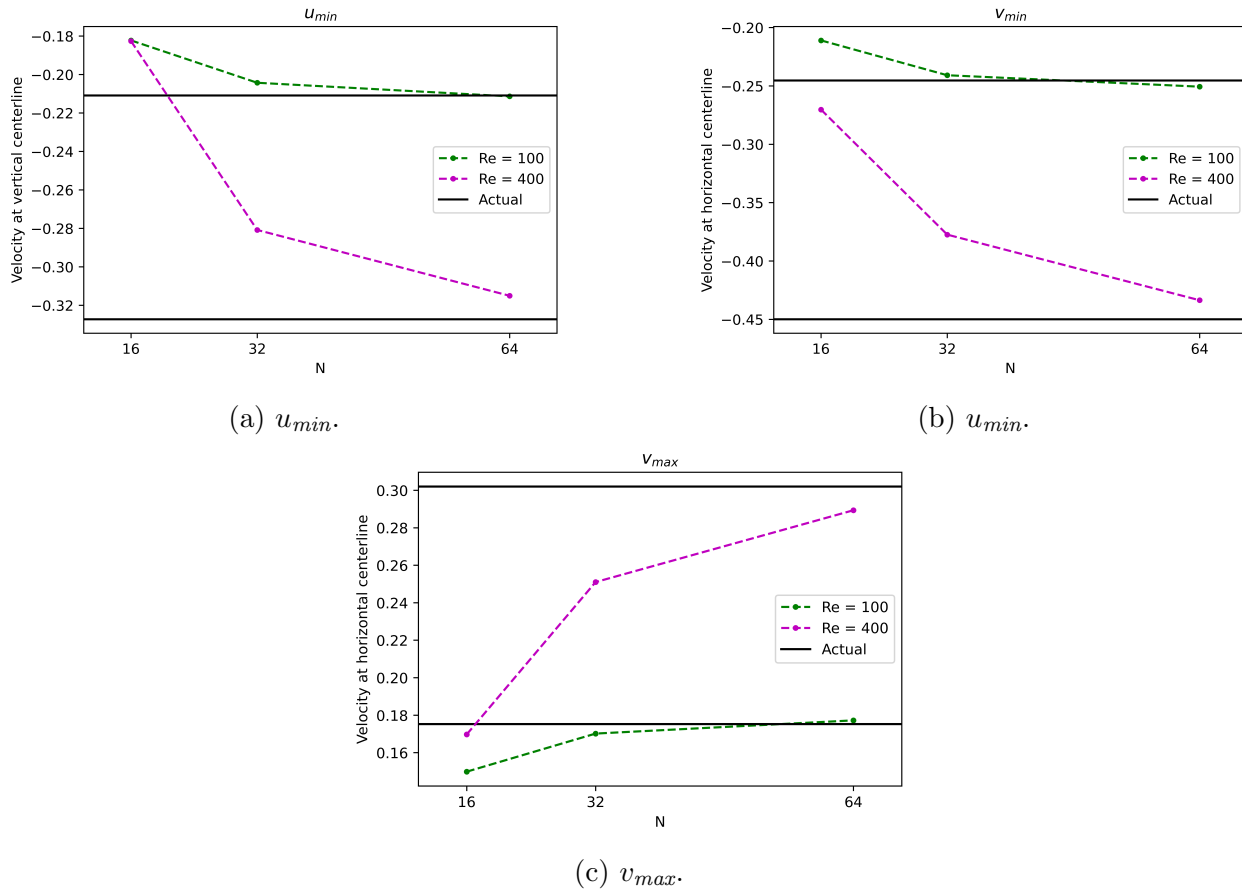


Figure 7: Comparison of velocities from centerline profiles.

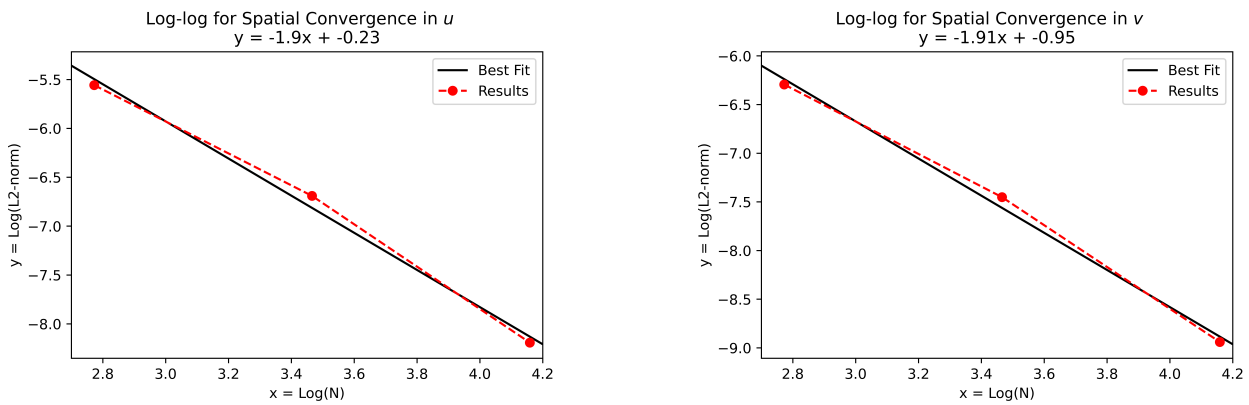
The general trend of the plots in Fig.7 is that the minimum and maximum velocities of the centerline plots are nearing the literature values as the grid size N is increased. It is notable that the higher Reynolds solutions require larger N to be as close to the literature result as for the smaller Reynolds solutions. This finding agrees with the differences in magnitude of percent error in Table 1.

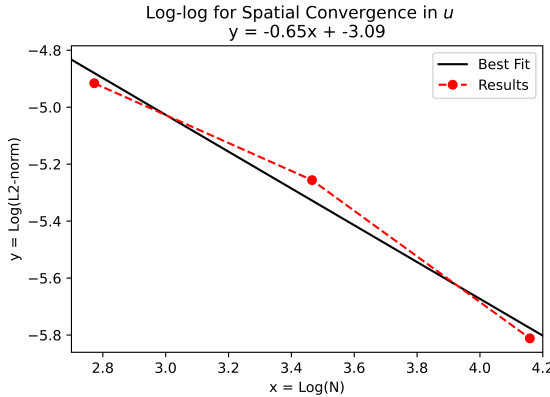
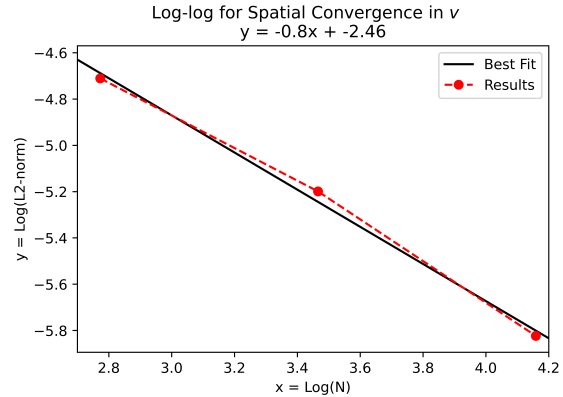
- (f) **Numerically compute the spatial convergence rate of your scheme. Detail how you computed the spatial convergence rate. Does it match what is expected based on your discretization.**

We take the L2 norm over the sum of all differences in velocities u or v between the grids with $N = \{16, 32, 64\}$ points and the solution with 128 grid points as the spatial error measurement. Since the values at the boundaries are constant between solutions, making the differences in solutions zero along the boundary, $(N - 2)^2$ points on the grid provide meaningful data and are used to compute the error.

$$\epsilon|_u = \frac{\sqrt{\sum_{i,j} (u_N - u_{128})_{ij}^2}}{(N - 2)^2} \quad (30)$$

To execute this, the solution of the grid with 128 points is restricted to match the grid sizes $N = \{16, 32, 64\}$. Meaning, the results from the finer grid are interpolated to a coarser grid. A restriction function was created which implements the boundary conditions for u, v and then averages the 8 fine mesh neighbors of the coarse point (N, S, E, W, NE, NW, SE, SW) in 2D, restricting the grid to a $N/2$ mesh. The 128 point grid was first restricted to $N = 64$, then it was recycled into the function to get the restriction at $N = 32$. The function was executed once more to restrict the 128 point grid to $N = 16$.

(a) Velocity u , Convergence rate = 1.9.(b) Velocity v , Convergence rate = 1.91.Figure 8: Spatial convergence in u and v at $Re = 100$.

(a) Velocity u , Convergence rate = 0.65.(b) Velocity v , Convergence rate = 0.80.Figure 9: Spatial convergence in u and v at $Re = 400$.

The spatial convergence rates for u and v are both approximately 2 for $Re = 100$ (Fig.8). This agrees with what we would expect for the spatial convergence rate when using central differences for the discretization. On the other hand, the convergence rates at $Re = 400$ are 0.65 and 0.80 (Fig.9), which do not match what is expected based on the discretization. This signifies that the choice of Reynolds number affects the rate at which the numerical solution spatially converges, such that higher Reynolds number may have a slower spatial convergence rate.